

Electronic Supporting information

Synthesis and characterization of Ag_2S and $\text{Ag}_2\text{S}/\text{Ag}_2(\text{S},\text{Se})$ NIR nanocrystals

Diego Ruiz,^a Martín Mizrahi,^b Harrison D. A. Santos,^{c,d} Daniel Jaque,^c Callum M.S. Jones,^e José Marqués-Hueso,^e Carlos Jacinto,^d Félix G. Requejo,^b Almudena Torres-Pardo,^f Jose M. González-Calbet^{f,g} and Beatriz H. Juárez^{*a,h}

^a IMDEA Nanoscience, Faraday 9, Campus de Cantoblanco, 28049, Madrid, Spain.

^b Instituto de Investigaciones Fisicoquímicas Teóricas y Aplicadas (INIFTA), CONICET and FCE, UNLP, CC/16, suc 4, 1900, La Plata, Argentina

^c Fluorescence Imaging Group, Materials Physics Department, Universidad Autónoma de Madrid, Campus Cantoblanco, 28049, Madrid, Spain.

^d Group of Nano-Photonics and Imaging, Instituto de Física, Universidade Federal de Alagoas, 57072-900 Maceió-AL, Brazil.

^e Institute of Sensors, Signals and Systems, Heriot-Watt University, Edinburgh, EH14 4AS, United Kingdom.

^f Inorganic Chemistry department, Chemical Sciences Faculty, Universidad Complutense de Madrid, 28040, Madrid, Spain.

^g ICTS National Center for Electronic Microscopy, Universidad Complutense, 28040, Madrid, Spain.

^h Department of Applied Physical Chemistry and Condensed Matter Physics Center (IFIMAC) Universidad Autónoma de Madrid, 28049 Madrid, Spain.

Section S1. Summary of the synthetic routes and the optical properties reported for Ag₂S NCs

Route	Silver precursor	Sulfur precursor	Solvent	Ligand(s)	Synthesis T (°C)	PL (nm)	PLQY	PL lifetime/ns	Ref.
Heat-up	AgDDTC	DT	DT	DT	200	975-1175	not shown	57-181	1
Heat-up	AgDDTC	DT	DT	DT, PEG-DHLA	200	1200	15.5% (water)	not shown	2
Heat-up	AgDDTC	DT	DT	DT, C18PMH-PEG	150	1100	17% (water)	61	3
Heat-up	AgDDTC	DT	ODE	DT, DSPE-PEG ₂₀₀₀	170	1170	4.48% (water)	not shown	4
Heat-up	AgDDTC	AgDDTC	ODE	OA, ODA	200	1058	not shown	not shown	5
Heat-up	AgDDTC	DT	ODE	DT, polypeptide gels	140	1100	5.1% (organic), 4.3% (water)	not shown	6
Heat-up	AgAc	DT	ODE	OLA	250	1250	not shown	not shown	7
Hot injection	AgAc	TMS	OT	OT	165	1150	4.5% (hexane)	not shown	8
Seeded growth	AgAc, AgOA	TMS	ODE, TOL	MA, OA	50-110	700-1250	0.18% (hexane), 0.15% (water)	57	9
Heat-up	AgOA	DT	ODE, OA	DT	220	1250	not shown	not shown	10
Hot injection	NHC-AgBr	TMS	CH ₂ Cl ₂ , ODE	NHC	RT	not shown	not shown	not shown	11
Hot injection	AgCl	(NH ₄) ₂ S	TOP	OLA	30	980	not shown	not shown	12
Heat-up	AgSCOPh	AgSCOPh	TOP, HDA, OCTA, DOA, EDA	HDA, OCTA, DOA, EDA	80-120	not shown	not shown	not shown	13
Hot injection	AgNO ₃	S in TOL	TOL	OCTA	RT	1000-1250	not shown	not shown	14
Hot injection	AgNO ₃	TAA in OLA	TOP	OLA	100	800	not shown	56.4	15
Heat-up	AgNO ₃	3-MPA	EG	3-MPA	145	510-1210	2.1% (water)	not shown	16
Hot injection	AgNO ₃	Na ₂ S	H ₂ O	BSA	37	650-850	0.75%-1.8% (water)	728	17
Heat-up	AgNO ₃	Na ₂ S	H ₂ O	2-MPA	30-90	786-950	14-39% (water)	not shown	18
Heat-up	AgNO ₃	Na ₂ S	H ₂ O	HSA	55	1060	1.26-1.32% (water)	not shown	19
Heat-up	AgNO ₃	S in NH ₂ -NH ₂	H ₂ O	GSH	RT	620	1.9% (water)	not shown	20
Heat-up	AgNO ₃	S in NH ₂ -NH ₂	H ₂ O	GSH	20	600-760	0.1-1.2% (water)	not shown	21
Hot injection	AgNO ₃	S in TOP	ODE	OA, ODA, TOP	150	not shown	not shown	not shown	22
Heat-up	AgNO ₃	DMSA	H ₂ O	DMSA	70-90	780-920	6.3-6.5% (water)	not shown	23
Hot injection	AgNO ₃	S in NH ₂ -NH ₂	H ₂ O	Multidentate polymers	95	687-1096	14.2-16.4% (water)	not shown	24
Heat-up	AgNO ₃	DT	DT	DT	200	not shown	not shown	not shown	25
Hot injection	AgNO ₃	S powder	ODA	ODA	170	not shown	not shown	not shown	26
Hot injection	AgNO ₃	TAA	OLA	OLA	210	1200	not shown	not shown	27
Hot injection	AgNO ₃	Na ₂ S	H ₂ O	MPEG-SH	90	775-930	1.9-65.6% (water)	not shown	28
Heat-up	AgNO ₃	DPA	H ₂ O	DPA	Micro wave IR	639-802	0.72-2.7% (water)	816	29

Abbreviations: DHLA: Dihydrolipoic acid, C18PMH-PEG: Poly(maleic anhydride-alt-1-octadecene)-polyethylene glycol, DSPE: distearoylphosphatidylethanolamine-poly(ethylene glycol), ODA: Octadecylamine, OA: Oleic acid, OLA: Oleylamine, TMS: bis(trimethylsilyl) sulfide, OT: 1-octanethiol, AgAc: Silver (I) acetate, AgOA: Silver (I) oleate, TOL: Toluene, MA: Myristic acid, NHC-AgBr: N-heterocyclic carbene-silver bromide, TOP: Trioctylphosphine, AgSCOPh: Silver (I) thiobenzoate, HDA: Hexadecylamine, OCTA: Octylamine, DOA: Dioctylamine, EDA: Ethylenediamine, 3-MPA: 3-mercaptopropionic acid, EG: Ethylene glycol, BSA: Bovine serum albumin, 2-MPA: 2-mercaptopropionic acid, HSA: Human serum albumin, DMSA: Dimercaptosuccinic acid, TAA: Thioacetamide, MPEG-SH: Thiol modified polyethylene glycol, DPA: D-penicillamine.

Table S1. Synthetic routes reported for Ag₂S NCs

Section S2. Experimental section

Chemicals: Silver (I) diethyldithiocarbamate (AgDDTC, 99%), 1-dodecanethiol (DT, >98%), toluene (TOL, 99.8%), acetone (technical grade), oleylamine (OLA, 70%), sulfur powder (S, synthesis grade), polyethylene glycol methyl ether thiol (PEG-SH, average M_n 6000), chloroform (CHCl_3 , >99.8%), tetrachloroethylene (TCE, >99%), trioctylamine (TOA, 98%), silver (I) nitrate (AgNO_3 , >99.0%), acetonitrile (99.8%), deuterated chloroform (CDCl_3 , 99.8% D), hexane (reagent grade), ethanol (EtOH, 96%), selenium powder (Se, 99.99%) and trioctylphosphine (TOP, 97%). All chemicals were used without further purification. The commercial Ag_2S -PEG-COOH NCs were purchased from NIR-optics technologies, China.

Syntheses of Ag_2S NCs by heat-up routes (route A):

For the synthesis of these NCs the route followed was the one by Zhang et al.² Briefly, 0.1 mmol of AgDDTC was added along with 10 mg of DT in a three neck round bottom flask. The mixture was heated to 200°C and left to react for an hour. The NCs were washed with ethanol and toluene.

Syntheses of Ag_2S NCs by hot injection (route B):

In this case, 0.2 mmol of AgDDTC, 60 mmol of DT and 10 ml of toluene were mixed in a three neck round bottom flask. The mixture was heated to 100°C and when the silver salt is completely dissolved and the solution turns to a bright yellow color 100 μL of a solution of 0.4 mmol of sulfur powder in 1 ml of OLA is swiftly injected. The solution is then left to react until it is quenched using a water bath. The content is passed to a plastic centrifuge tube and precipitated with acetone.

These NCs were found to be very stable in the reaction media, so several cycles of centrifugation at 9000 rpm and cooling of the centrifuge tube were necessary to precipitate all the NCs. The addition of ethanol has a positive influence in the destabilization of the NCs but it was also found to irrevocably quench the NCs PL almost completely. Typically, the washing steps were carried out using the same amount of acetone as the reaction media and a few drops of ethanol if the NCs were too stable to precipitate.

Syntheses of $\text{Ag}_2\text{S}/\text{Ag}_2(\text{S},\text{Se})$ NCs:

For the synthesis of these NCs: 0.2 mmol of AgDDTC, 60 mmol of DT and 10 ml of toluene were mixed in a three neck round bottom flask. The mixture was heated to 100°C and when the silver salt is completely dissolved and the solution turns to a bright yellow color 100 μL of a solution of 0.4 mmol of sulfur powder in 1 ml of OLA is swiftly injected.

After 5 minutes 100 μL of a 1 M solution of Se powder in TOP is injected into the NCs dispersion. The solution is left to react for 10 minutes and then, it is left to naturally cool to room temperature. The washing steps were carried out with acetone and chloroform.

Ligand exchange reactions:

All batches are dispersed in 10 ml of chloroform and from that solution, 1 ml of NCs ($[\text{Ag}^+] \cong 1.5 \text{ mg/ml}$) is added to a 5 ml chloroform solution containing 100 mg of PEG-SH. The mixture is sonicated at room temperature for half an hour and then is left in a mechanical agitator for 1.5 h. After that, the chloroform is blown dry using a N_2 flow and 5-10 ml of ethanol is added to the NCs deposit. The solution is vortexed and sonicated until an optically clear dispersion is obtained. In order to remove the excess polymer two centrifugation steps were followed with ethanol using Sartorius Vivaspin 20 MWCO= 100 KDa ultracentrifugation tubes. After that, three cycles of centrifugation and redispersion in water were found to be enough to eliminate the ethanol and the remaining polymer. The NCs obtained using this method were stable in the water dispersion for months in storage at 4°C.

In order to compare the behavior of the two kinds of NCs in ligands exchange reactions, aliquots with the same quantity of Ag^+ (measured by ICP-MS) were subjected to the above procedure. The amount of NCs transferred to water were measured as the quantity of Ag^+ detected in the water samples measured using ICP-MS.

Photoluminescence Quantum Yield measurements

Fluorescence spectra were obtained using a calibrated spectrofluorometer (Edinburgh Instruments, FLS920), with a xenon lamp as excitation source, an integrating sphere (Jobin-Yvon), and a liquid nitrogen cooled NIR photomultiplier tube (Hamamatsu, R5509-72).

Synchrotron measurements

X-ray absorption spectroscopy (XAS) experiments were performed at the SXS (S K- and Ag L_3 - edges) and XAFS2 (Se K-edge) beamlines at the LNLS (Laboratório Nacional de Luz Síncrotron), Campinas, Brazil.

X-ray Absorption Near Edge Structure (XANES) spectroscopy measurements at the S K-edge (2472 eV) and Ag L₃-edge (3351 eV) were carried out using a InSb(111) double-crystal monochromator, giving an energy resolution of 2 eV at the S K-edge, and 1 eV at the Ag L₃-edge. Experiments with soft X-rays were performed in a vacuum chamber at 10⁻⁹ mbar and room temperature (RT). The incident beam intensity (I_0) was measured using a thin foil of Al. Samples were dropped on carbon tapes to be measured in Total Electron Yield (TEY) and Fluorescence (FL) modes simultaneously. The photon energies were calibrated using a Mo and Ag metallic foil setting the first inflection point of the Mo L₃ absorption edge at 2520 eV for S, and to the Ag L₃ absorption edge (3351 eV) for Ag measurements. The final XANES spectra were obtained after background subtraction and normalization to the postedge intensity.

XANES and Extended X-ray Absorption Fine Structure (EXAFS) experiments at the Se K-edge (12658 eV) were measured at room temperature using a Si(111) single channel-cut crystal monochromator in fluorescence mode. An ionization chamber was used to detect the incident flux and a 15-element germanium solid-state detector was used to sense the fluorescence signal from the sample. The EXAFS data was extracted from the measured absorption spectra by standard methods using the ATHENA software which is part of the Demeter package.³⁰ The Fourier transforms were calculated using the Hanning filtering function. EXAFS modeling was carried out using the ARTEMIS program (Demeter package). Structural parameters (coordination numbers, interatomic distances and Debye–Waller factor) were obtained by nonlinear least-squares fit of the theoretical EXAFS signal to the data in R space by Fourier Transforming both the experimental and calculated data. Theoretical scattering path amplitudes and phase shifts for all paths used on the fits and simulations were calculated using the FEFF code.³¹ The passive reduction factor S_0^2 was restrained to the value of 0.72. This value was obtained fitting the EXAFS spectrum of metallic Se foil and constraining the coordination number of the first coordination shell to 2.

NMR experiments

NMR samples were thoroughly washed and dried using a N₂ flux to minimize the signals of the solvent and non-solvent used in the washing steps. ¹H NMR spectra were recorded using a Bruker Avance II 300 MHz spectrometer. DOSY experiments were recorded using a Bruker Avanced III-HD NANOBAV 300 MHz with diffusion time of 250 ms and a variable gradient length.

TEM characterization:

Figures 1A and 1B were acquired in a JEOL 1010 operating at 100 kV. Images 1C-1I were acquired in an aberration-corrected JEOL-JEM ARM300cF microscope operating at 80 kV in order to minimize the electron beam damage.

Section S3. Characterization of route A NCs

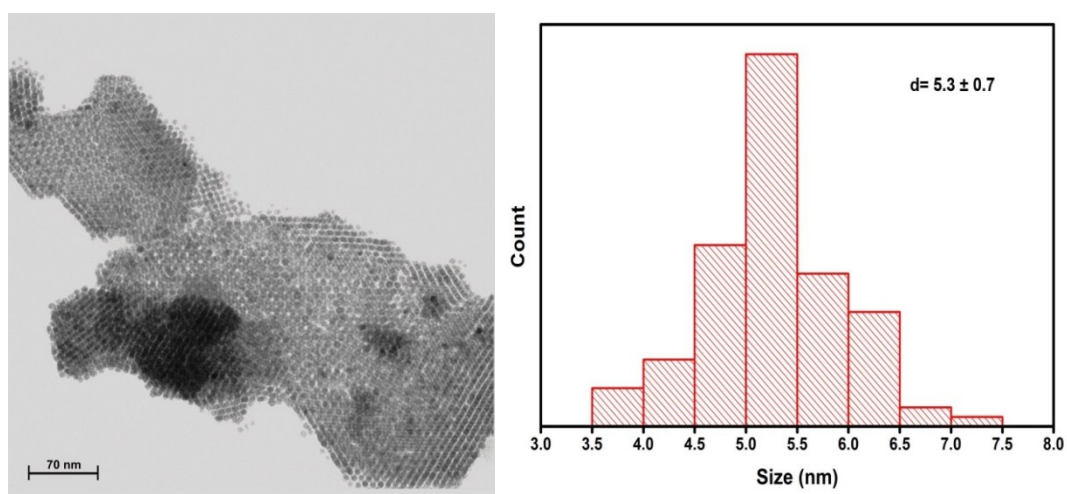


Figure S1. TEM image and size distribution of the route A as-synthesized Ag_2S NCs

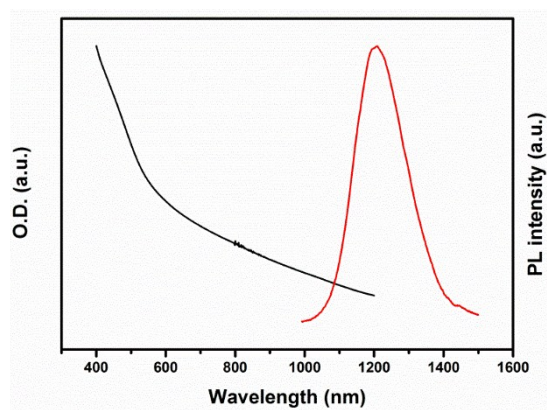


Figure S2. Steady-state absorption and PL of the route A, Ag_2S NCs

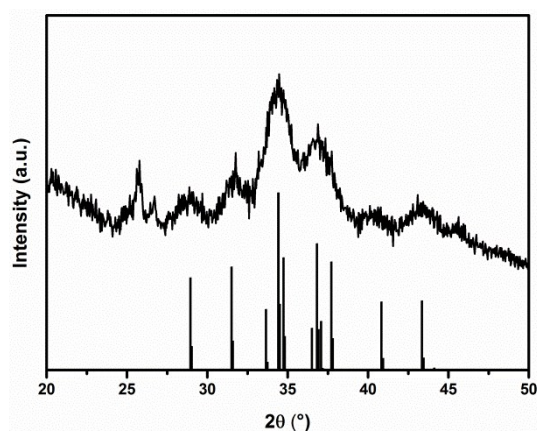


Figure S3. XRD diffractogram of the Ag_2S NCs synthesized by route A

Section S4. Identification of the $\text{AgSC}_{12}\text{H}_{25}$ polymer during the course of the reaction

Isolation of the intermediate silver compound: In order to isolate the chemical compound that undergoes the decomposition to Ag_2S a mixture of 0.2 mmol of AgDDTC , 60 mmol of DT and 10 ml of toluene is heated to 100°C in a three neck round bottom flask. When the silver salt is completely dissolved and the reaction media presents a bright yellow color the reaction is quenched using a water bath. Upon cooling, the reaction starts to present turbidity and a darker color, due a partial decomposition of the precursor. The white solid is isolated from the reddish liquid by centrifugation and washed with hexane. Figure S4 compares a TEM image of this product with the NCs aggregates obtained by the heat-up route (route A).

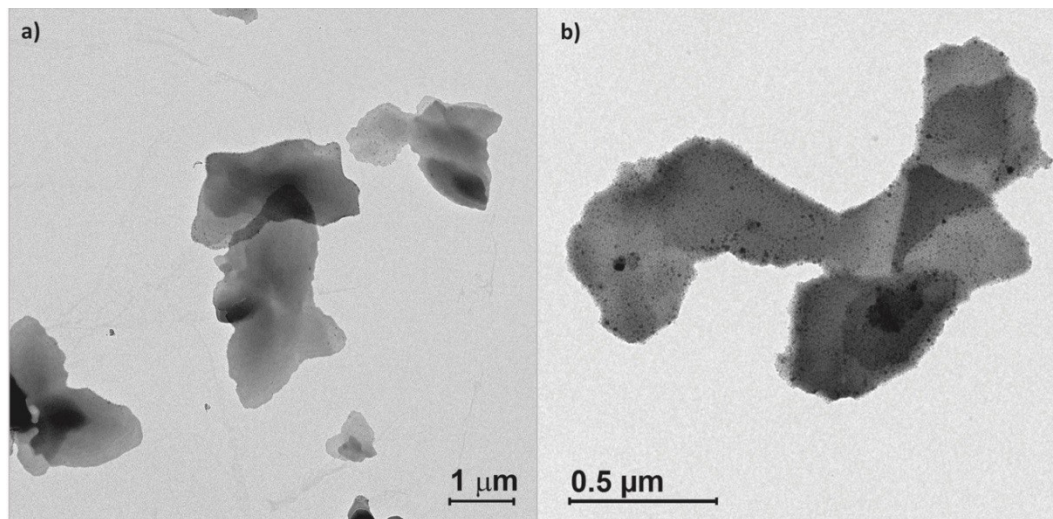


Figure S4. a) TEM image of $\text{AgSC}_{12}\text{H}_{25}$ lamellae isolated from the reaction media and b) Aggregates of Ag_2S NCs synthesized by heat-up route A.

The presence of the $\text{AgSC}_{12}\text{H}_{25}$ in the reaction media was confirmed also using a series of XRD experiments. Figure S5 compares the XRD diffractogram of the starting silver salt, AgDDTC , with the XRD of the intermediate isolated from the heat-up reaction and the polymer $\text{AgSC}_{12}\text{H}_{25}$ synthesized as described below. It can be seen that the peaks of the intermediate match clearly with those of the lamellar structure of the silver polymer, and are significantly different from those corresponding to the initial salt precursor.

Synthesis of $\text{AgSC}_{12}\text{H}_{25}$: The synthesis of the silver polymer was carried out based on a previously reported procedure.³² A solution of 1 mmol of AgNO_3 in 5 ml of acetonitrile is slowly injected into a solution of 2 mmol of 1-dodecanethiol and 2 mmol of trioctylamine in 10 ml of acetonitrile. The $\text{AgSC}_{12}\text{H}_{25}$ is formed immediately upon the injection of the silver solution. The white powder is washed by centrifugation in hexane to eliminate the excess products and dried using an oven at 50°C .

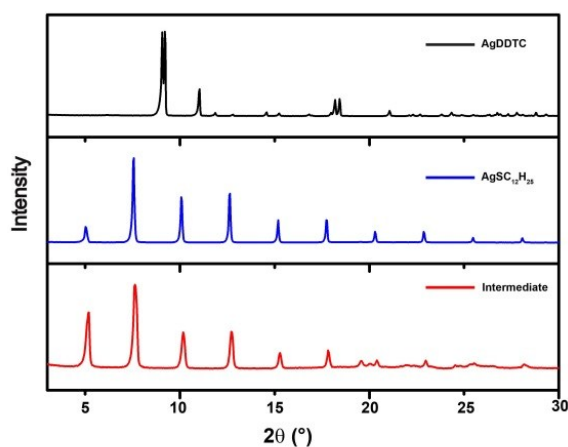


Figure S5. XRD diffractograms of the AgDDTC , $\text{AgSC}_{12}\text{H}_{25}$ and the reaction intermediate

Section S5. Characterization of the Ag₂S NCs synthesized by route B

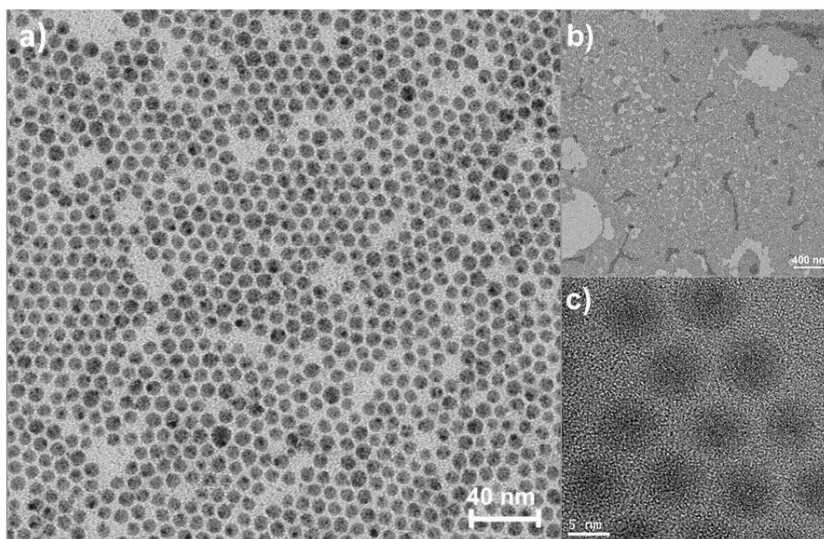


Figure S6. TEM and HRTEM images of Ag₂S NCs synthesized by route B at different magnifications

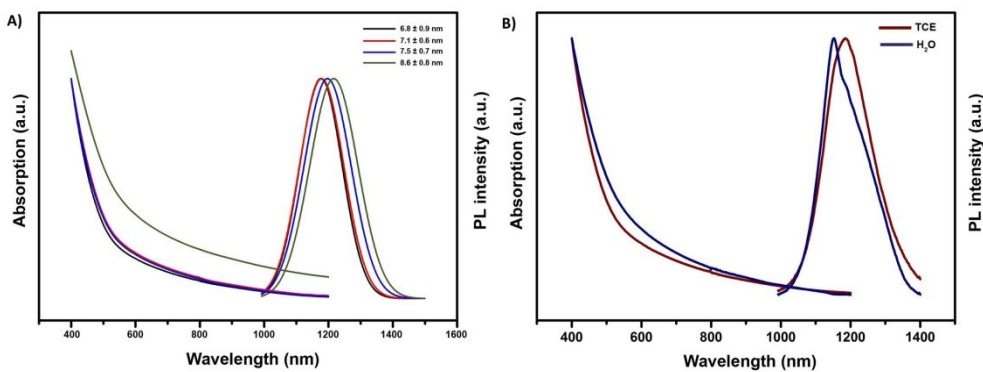


Figure S7. a) Optical extinction and photoluminescence spectra of different aliquots of Ag₂S NCs with different sizes (specified in the legend) and b) optical absorption and photoluminescence spectra before (dark red) and after (dark blue) the ligand exchange procedure described in section S2. Red line corresponds to NCs in tetrachloroethylene (TCE) and blue line for NCs transferred to water.

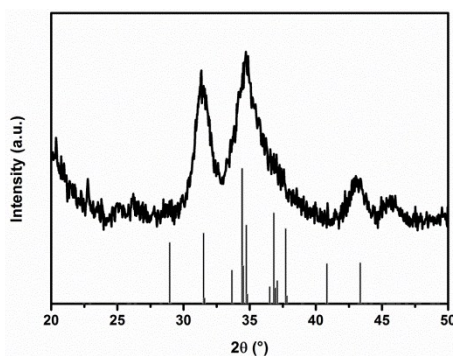


Figure S8. XRD diffractogram of the Ag₂S NCs synthesized by route B

Section S6. Characterization of $\text{Ag}_2\text{S}/\text{Ag}_2(\text{S,Se})$ NCs

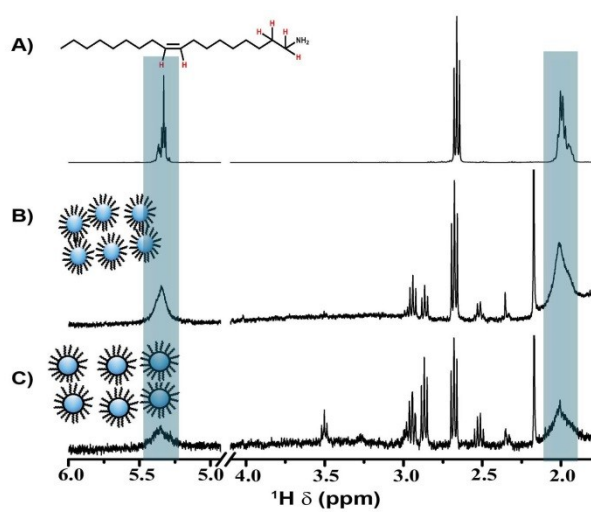


Figure S9. ^1H NMR spectra of a) OLA, b) route B Ag_2S NCs, and c) $\text{Ag}_2\text{S}/\text{Ag}_2(\text{S,Se})$ NCs.

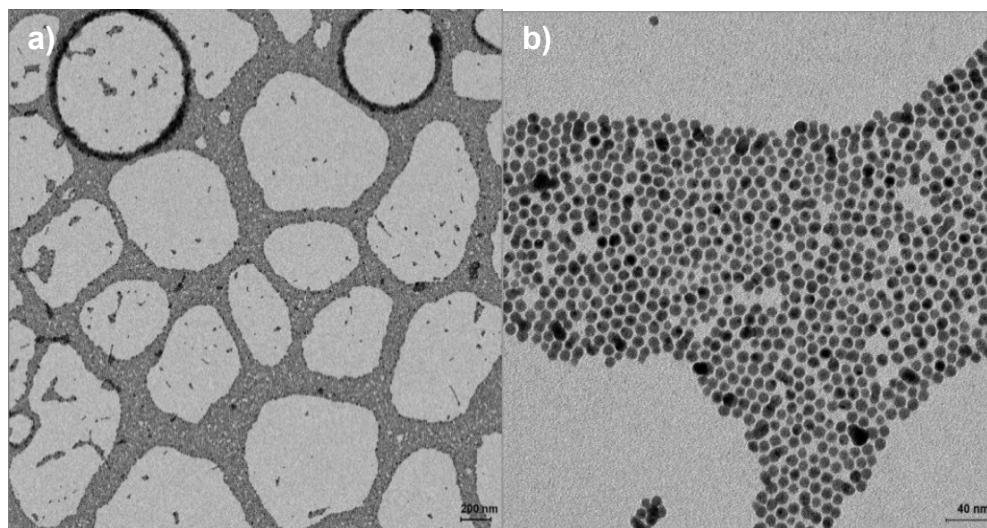


Figure S10. TEM images of the as-synthesized $\text{Ag}_2\text{S}/\text{Ag}_2(\text{S,Se})$ NCs.

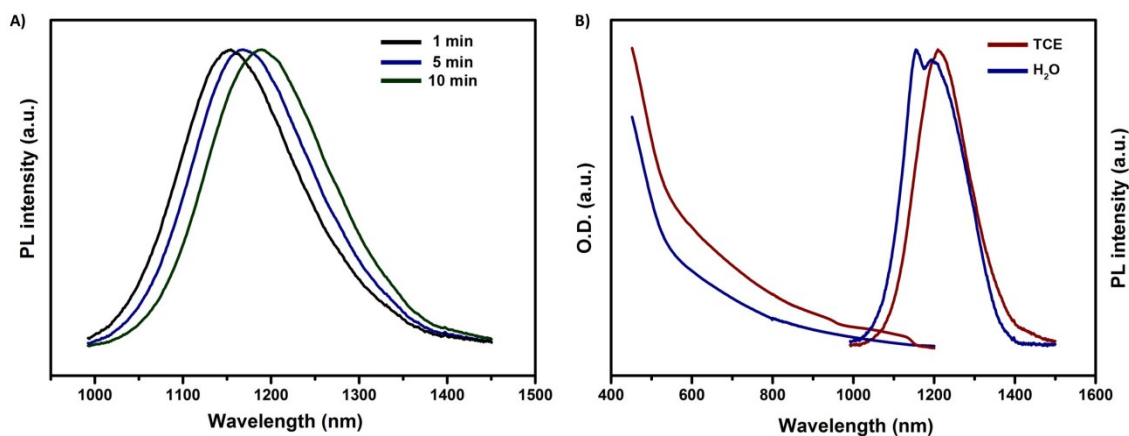


Figure S11. a) Photoluminescence spectra of aliquots of the $\text{Ag}_2\text{S}/\text{Ag}_2(\text{S,Se})$ NCs at different reaction times after the Se@TOP injection and b) Absorption and photoluminescence spectra of the NCs before (dark blue) and after the ligand exchange procedure (dark red).

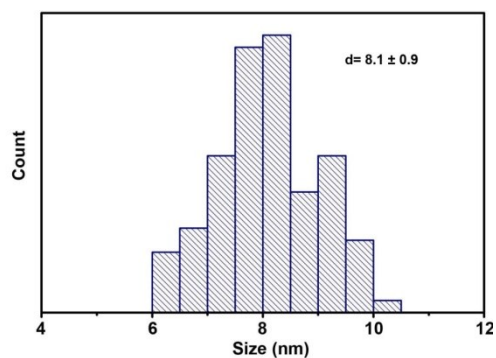


Figure S12. Size distribution of the as-synthesized $\text{Ag}_2\text{S}/\text{Ag}_2(\text{S,Se})$ NCs

Section S7. Structural parameters from EXAFS analysis of the Se K-edge

Sample	N _{Se-Ag}	R _{Se-Ag} (Å)	DWF _{Se-Ag} (Å ²)	N _{Se-S}	R _{Se-S} (Å)	DWF _{Se-S} (Å ²)
(Ag ₂ S/Ag ₂ (S,Se) NCs	2.8(4)	2.6 - 2.8	0.010(3)	1.0(4)	2.10(4)	0.06(1)
Ag ₂ S standard	7	2.7 - 2.9				

Table S2. Fitted structural parameters (N: average coordination number; R: interatomic distance; DWF: Debye-Waller factor) obtained from the EXAFS analysis using a two-shell model.

References

1. Y. Zhang, Y. Liu, C. Li, X. Chen and Q. Wang, *The Journal of Physical Chemistry C*, 2014, **118**, 4918-4923.
2. Y. Zhang, G. Hong, Y. Zhang, G. Chen, F. Li, H. Dai and Q. Wang, *ACS Nano*, 2012, **6**, 3695-3702.
3. F. Hu, C. Li, Y. Zhang, M. Wang, D. Wu and Q. Wang, *Nano Research*, 2015, **8**, 1637-1647.
4. M.-Y. Qin, X.-Q. Yang, K. Wang, X.-S. Zhang, J.-T. Song, M.-H. Yao, D.-M. Yan, B. Liu and Y.-D. Zhao, *Nanoscale*, 2015, **7**, 19484-19492.
5. Y. Du, B. Xu, T. Fu, M. Cai, F. Li, Y. Zhang and Q. Wang, *Journal of the American Chemical Society*, 2010, **132**, 1470-1471.
6. D.-H. Zhao, J. Yang, R.-X. Xia, M.-H. Yao, R.-M. Jin, Y.-D. Zhao and B. Liu, *Chemical Communications*, 2018, **54**, 527-530.
7. P.-J. Wu, J.-W. Yu, H.-J. Chao and J.-Y. Chang, *Chemistry of Materials*, 2014, **26**, 3485-3494.
8. H. He, Y. Lin, Z. Q. Tian, D. L. Zhu, Z. L. Zhang and D. W. Pang, *Small*, 2018, **14**, 1703296.
9. P. Jiang, Z.-Q. Tian, C.-N. Zhu, Z.-L. Zhang and D.-W. Pang, *Chemistry of Materials*, 2012, **24**, 3-5.
10. P. Li, Q. Peng and Y. Li, *Chemistry – A European Journal*, 2010, **17**, 941-946.
11. H. Lu and R. L. Brutchey, *Chemistry of Materials*, 2017, **29**, 1396-1403.
12. H. Zhang, B.-R. Hyun, F. W. Wise and R. D. Robinson, *Nano Letters*, 2012, **12**, 5856-5860.
13. W. P. Lim, Z. Zhang, H. Y. Low and W. S. Chin, *Angewandte Chemie International Edition*, 2004, **43**, 5685-5689.
14. H. Doh, S. Hwang and S. Kim, *Chemistry of Materials*, 2016, **28**, 8123-8127.
15. R. Ahmad, R. Srivastava, H. Bhardwaj, S. Yadav, V. Nand Singh, S. Chand, N. Singh and S. Sapra, *ChemistrySelect*, 2018, **3**, 5620-5629.
16. P. Jiang, C.-N. Zhu, Z.-L. Zhang, Z.-Q. Tian and D.-W. Pang, *Biomaterials*, 2012, **33**, 5130-5135.
17. Y. Wang and X.-P. Yan, *Chemical Communications*, 2013, **49**, 3324-3326.
18. I. Hocaoglu, M. N. Cizmeciyan, R. Erdem, C. Ozen, A. Kurt, A. Sennaroglu and H. Y. Acar, *Journal of Materials Chemistry*, 2012, **22**, 14674-14681.
19. T. Yang, Y. a. Tang, L. Liu, X. Lv, Q. Wang, H. Ke, Y. Deng, H. Yang, X. Yang, G. Liu, Y. Zhao and H. Chen, *ACS Nano*, 2017, **11**, 1848-1857.
20. L. Kong, W. Liu, X. Chu, Y. Yao, P. Zhu and X. Ling, *RSC Advances*, 2015, **5**, 80530-80535.
21. C. Wang, Y. Wang, L. Xu, D. Zhang, M. Liu, X. Li, H. Sun, Q. Lin and B. Yang, *Small*, 2012, **8**, 3137-3142.
22. A. Sahu, L. Qi, M. S. Kang, D. Deng and D. J. Norris, *Journal of the American Chemical Society*, 2011, **133**, 6509-6512.
23. I. Hocaoglu, F. Demir, O. Birer, A. Kiraz, C. Sevrin, C. Grandfils and H. Yagci Acar, *Nanoscale*, 2014, **6**, 11921-11931.
24. R. Gui, A. Wan, X. Liu, W. Yuan and H. Jin, *Nanoscale*, 2014, **6**, 5467-5473.
25. Z. Zhuang, X. Lu, Q. Peng and Y. Li, *Chemistry – A European Journal*, 2011, **17**, 10445-10452.
26. G. Zhu and Z. Xu, *Journal of the American Chemical Society*, 2011, **133**, 148-157.
27. Y. Wang, X. Li, M. Xu, K. Wang, H. Zhu, W. Zhao, J. Yan and Z. Zhang, *Nanoscale*, 2018, **10**, 2577-2587.
28. D. Asik, M. B. Yagci, F. Demir Duman and H. Yagci Acar, *Journal of Materials Chemistry B*, 2016, **4**, 1941-1950.
29. X. Jia, D. Li, J. Li and E. Wang, *RSC Advances*, 2015, **5**, 80929-80932.
30. B. Ravel and M. Newville, *Journal of Synchrotron Radiation*, 2005, **12**, 537-541.
31. J. J. Rehr, J. J. Kas, F. D. Vila, M. P. Prange and K. Jorissen, *Physical Chemistry Chemical Physics*, 2010, **12**, 5503-5513.
32. I. G. Dance, K. J. Fisher, R. M. H. Banda and M. L. Scudder, *Inorganic Chemistry*, 1991, **30**, 183-187.